EUROPEAN ORGANIZATION FOR NUCLEAR RESEARCH

CERN-EP/2000-057
April 28, 2000

Search for Anomalous $\mathbf{ZZ\gamma}$ and $\mathbf{Z\gamma\gamma}$ couplings in the process $\mathbf{e^+e^- \rightarrow Z\gamma}$ at LEP

The L3 Collaboration

Abstract

We search for anomalous trilinear gauge couplings in the $\mathrm{ZZ}\gamma$ and $\mathrm{Z}\gamma\gamma$ vertices using data collected with the L3 detector at LEP at a centre–of–mass energy $\sqrt{s} =$ 189 GeV. No evidence is found and limits on these couplings and on new physics scales are derived from the analysis of the process $\mathrm{e^+e^-} \rightarrow \mathrm{Z}\gamma$.

Submitted to *Phys. Lett. B*

Introduction

The process $e^+e^- \to Z\gamma$ is interesting to test the existence of new physics [1]. In particular, the existence of anomalous couplings between neutral gauge bosons can be probed by means of this reaction. Effects coming from $ZZ\gamma$ and $Z\gamma\gamma$ couplings are expected to be very small in the Standard Model [1,2], but can be enhanced in compositeness models [3,4] or if new particles enter in higher order corrections.

Assuming only Lorentz and $U(1)_{em}$ gauge invariance, the most general form of the $ZZ\gamma$ and $Z\gamma\gamma$ vertices can be parametrized by means of eight anomalous couplings. The couplings are: h_i^V ($i = 1$ to $4; V = \gamma, Z$), where a V superscript corresponds to a $ZV\gamma$ vertex. The couplings h_1^V and h_2^V are CP violating whereas h_3^V and h_4^V are CP conserving. The anomalous couplings contribution to the $Z\gamma$ cross section increases with the centre–of–mass energy, $\sqrt{s}$, while the Standard Model contribution decreases. All these couplings are zero at tree level in the Standard Model, and only the CP conserving ones receive a small contribution ($\approx 10^{-4}$) at the one loop level [1,2]. An alternative parametrization, which introduces the energy scales of new physics Λ_{iV} is [5]:

$$\frac{\sqrt{\alpha}\ h_i^V}{m_Z^2} \equiv \frac{1}{\Lambda_{iV}^2} \quad , i = 1, 3 \tag{1}$$

$$\frac{\sqrt{\alpha}\ h_i^V}{m_Z^4} \equiv \frac{1}{\Lambda_{iV}^4} \quad , i = 2, 4. \tag{2}$$

The anomalous couplings h_i^V cannot get arbitrarily large values due to unitarity constraints, and should vanish when $s \to \infty$ [6,7]. For hadron colliders, this means that a form factor dependence should be used [7–10], because the effective centre–of–mass energy of the collision is variable. For e^+e^- colliders, the centre–of–mass energy is fixed and no form factors are needed [11]. Therefore, the results are model independent and no hypothesis about the behaviour close to the new physics scale is made [11,12]. The main effects of anomalous $ZZ\gamma$ and $Z\gamma\gamma$ couplings are an increase of the $Z\gamma$ total cross section and a modification of the differential spectrum of the photon, mainly at large polar angles. Limits on $ZZ\gamma$ and $Z\gamma\gamma$ couplings have been published at the Tevatron [8–10] and LEP [13,14].

Data collected by the L3 detector [15] in 1998 at $\sqrt{s} = 189$ GeV, amounting to 176 pb^{-1} of integrated luminosity, are used to study the anomalous couplings $ZZ\gamma$ and $Z\gamma\gamma$ in the channels $e^+e^- \to q\bar{q}\gamma$ and $e^+e^- \to \nu\bar{\nu}\gamma$. In this article, a new calculation [11] is used.[1)] The results presented in this paper supersede our previous results [13] due to the higher $\sqrt{s}$ and integrated luminosity, which improve the sensitivity, and to the new calculation used.

Event Selection

The main signature of the process $e^+e^- \to Z\gamma$ is the production of a photon of high energy, E_γ. A photon candidate is identified as a shower in the BGO electromagnetic barrel or end-cap calorimeters with more than 90% of its energy deposited in a 3×3 crystal matrix. The mass of the system recoiling against the photon, $m_{rec} = (s - 2E_\gamma\sqrt{s})^{1/2}$, is required to satisfy 80 GeV $< m_{rec} <$ 110 GeV, and thus is consistent with that of a Z. For the $\sqrt{s}$ value considered,

[1)]Previous publications use reference [16] as the theoretical input, however recently [11] an error in the formulation was found. Thus previous limits cannot be directly compared with those obtained in this paper.

Process	$\mathcal{L}$ (pb^{-1})	ϵ (%)	Events	σ (pb)	$\sigma_{\rm SM}$ (pb)
$\rm e^+e^- \rightarrow q\bar{q}\gamma$	172.1	28.9 ± 0.1	899	18.1 ± 0.6	17.9
$\rm e^+e^- \rightarrow \nu\bar{\nu}\gamma$	175.6	33.6 ± 0.2	288	4.8 ± 0.3	5.0

Table 1: Integrated luminosities, $\mathcal{L}$, efficiencies, ϵ, of the selection, number of selected events and measured cross sections. The error on the efficiencies accounts for Monte Carlo statistics. The corresponding Standard Model cross sections $\sigma_{\rm SM}$ [17, 18] are also listed.

the cuts on the recoiling mass correspond to an energy of the photon between 62 GeV and 78 GeV.

In the estimation of signal and background processes the following Monte Carlo generators have been used: KK2F [17] for $\rm e^+e^- \rightarrow q\bar{q}\gamma$, $\rm e^+e^- \rightarrow q\bar{q}$, KORALZ [18] for $\rm e^+e^- \rightarrow \nu\bar{\nu}\gamma$, EXCALIBUR [19] for four fermion final states, DIAG36 [20] for $\rm e^+e^- \rightarrow e^+e^-e^+e^-$, BHWIDE [21] and TEEGG [22] for $\rm e^+e^- \rightarrow e^+e^-\gamma(\gamma)$. All generated events are passed through a simulation of the L3 detector response [23] and through the same analysis procedure used for data. Time dependent inefficiencies are taken into account in the simulation procedure.

Cross sections and efficiencies are quoted within the following phase space cuts: at least one photon of energy greater than 20 GeV with polar angle in the range $5^\circ < \theta_\gamma < 175^\circ$.

Selection of $\rm e^+e^- \rightarrow q\bar{q}\gamma$ events

In addition to a photon candidate recoiling against a Z, high multiplicity and energy-momentum balance are required to select $\rm e^+e^- \rightarrow q\bar{q}\gamma$ events:

- The event must have more than 6 tracks and more than 11 calorimetric clusters.
- The transverse energy imbalance must be less than 15% of the visible energy, and the longitudinal energy imbalance less than 20% of the visible energy.
- Events are rejected if the photon candidate is isolated from the two jets and is associated with a track. This requirement eliminates a substantial contamination of $\rm e^+e^- \rightarrow We\nu \rightarrow q\bar{q}'e\nu$ and $\rm e^+e^- \rightarrow q\bar{q}e^+e^-$ events.
- The polar angle of the photon, θ_γ, must be in the range $|\cos\theta_\gamma| < 0.74$ or $0.82 < |\cos\theta_\gamma| < 0.97$.

Using these criteria, 899 events are selected. The trigger inefficiency is estimated to be negligible due to the redundancy of subtriggers involved in triggering this final state.

Three backgrounds are found to contribute: $\rm e^+e^- \rightarrow q\bar{q}'e\nu$ and $\rm e^+e^- \rightarrow q\bar{q}e^+e^-$, where one of the electrons fakes a photon, giving 0.5% and 0.4% contamination respectively, and $\rm e^+e^- \rightarrow q\bar{q}$ events, contributing to a 1.2% contamination, mainly due to photons from π^0.

The measured cross section for $\rm e^+e^- \rightarrow q\bar{q}\gamma$ is shown in Table 1 and is in agreement with the Standard Model expectation. Figures 1 and 2 show the recoiling mass distribution and the polar angle of the photon.

Selection of $\rm e^+e^- \rightarrow \nu\bar{\nu}\gamma$ events

In addition to the presence of a photon the selection criteria for the $\rm e^+e^- \rightarrow \nu\bar{\nu}\gamma$ channel require low activity in the detector and large energy-momentum imbalance.

- The event cannot have more than 10 calorimetric clusters. The number of hits in the tracking chamber associated to a calorimetric cluster must not exceed 40% of the expected number of hits for a charged track.

- The polar angle of the photon candidate must satisfy $|\cos\theta_\gamma| < 0.74$ or $0.82 < |\cos\theta_\gamma| < 0.96$.

- The energy imbalance transverse to the beam direction must be more than 20% of the visible energy, and the energy of the photon must be more than 95% of the visible energy.

- To suppress cosmic ray background, there must be at least one scintillator time measurement within ± 5 ns of the beam crossing time. The scintillator signals must be associated to calorimetric clusters.

A total of 288 events are selected. The trigger efficiency is estimated to be 93.5%, using an independent sample of data events.

The background in the selected sample is found to be negligible. The measured cross section for $\mathrm{e^+e^-} \to \nu\bar{\nu}\gamma$ is shown in Table 1. It is in agreement with the Standard Model expectation. Figure 3 shows the recoiling mass distribution and Figure 4 shows the polar angle of the photon.

Results

The analysis is performed by means of the "Optimal Variables" [24] approach. The differential cross section of the process $\mathrm{e^+e^-} \to \mathrm{Z}\gamma$ is written as a function of the anomalous couplings:

$$\frac{d\sigma}{d\vec{\Omega}} = c_0(\vec{\Omega}) + \sum_{i=1}^{4}\sum_{V=\gamma,\mathrm{Z}} c_{1,i}(\vec{\Omega}) h_i^V + \sum_{i=1}^{4}\sum_{V=\gamma,\mathrm{Z}}\sum_{j=1}^{4}\sum_{V'=\gamma,\mathrm{Z}} c_{2,ij}(\vec{\Omega}) h_i^V h_j^{V'}, \quad (3)$$

where $\vec{\Omega} = (E_\gamma, \theta_\gamma, \phi_\gamma, \theta_f^{\mathrm{Z}}, \phi_f^{\mathrm{Z}})$. E_γ, θ_γ and ϕ_γ are the energy and angular variables of the photon, and $\theta_f^{\mathrm{Z}}, \phi_f^{\mathrm{Z}}$ the angles of the fermion f in the Z rest frame. For the $\mathrm{e^+e^-} \to \nu\bar{\nu}\gamma$ case, the neutrino angular variables are integrated out, leaving three variables in the calculation. As the couplings are small, the quadratic term is neglected, and the optimal variable for each coupling is defined as:

$$\mathcal{O}_{1,i} \equiv \frac{c_{1,i}(\vec{\Omega})}{c_0(\vec{\Omega})}. \quad (4)$$

This method profits from having a one-dimensional parametrization which uses all the available kinematic information.

A binned maximum likelihood fit of the expected optimal variable distribution to the data is performed. A reweighting technique is used to compute the expected number of events in the presence of anomalous couplings. In these fits, only one coupling is fitted each time, keeping all the other couplings at zero. The distributions of the optimal variables for the couplings h_1^{Z} and h_4^γ are shown as an example in Figures 5 and 6, respectively.

No deviations from the Standard Model expectations are found. Both $\mathrm{q\bar{q}}\gamma$ and $\nu\bar{\nu}\gamma$ samples lead to the same results. The limits on the anomalous couplings at 95% confidence level (CL) coming from both samples are:

$$
\begin{array}{ll}
-0.26 < h_1^{\mathrm{Z}} < 0.09 & -0.20 < h_1^{\gamma} < 0.08 \\
-0.10 < h_2^{\mathrm{Z}} < 0.16 & -0.11 < h_2^{\gamma} < 0.11 \\
-0.26 < h_3^{\mathrm{Z}} < 0.21 & -0.11 < h_3^{\gamma} < 0.03 \\
-0.11 < h_4^{\mathrm{Z}} < 0.19 & -0.02 < h_4^{\gamma} < 0.10.
\end{array}
$$

An independent analysis using a maximum likelihood fit in the five-dimensional phase space, described in our previous publication [13] is also performed as a cross check. The results obtained using this method are compatible with those obtained with the optimal variables.

Fits to the two-dimensional distributions of the optimal observables are performed to determine the pairs of the CP-violating and CP-conserving couplings, keeping in each case the other couplings fixed at zero. Results at 95% CL are shown in Table 2. There exists a strong correlation between the fitted values of the CP-violating couplings (h_1^V, h_2^V) or CP-conserving couplings (h_3^V, h_4^V). Contours for 95% CL two-dimensional limits on each pair of couplings, for $\mathrm{ZZ}\gamma$ and $\mathrm{Z}\gamma\gamma$, are shown in Figures 7 and 8.

Parameter	Fitted value	Negative limits	Positive limits	Correlation coefficient
h_1^{Z}	−0.17	−0.72	0.45	0.94
h_2^{Z}	−0.09	−0.49	0.36	
h_3^{Z}	−0.01	−0.76	0.67	0.95
h_4^{Z}	0.00	−0.49	0.49	
h_1^{γ}	−0.07	−0.36	0.24	0.88
h_2^{γ}	−0.04	−0.25	0.17	
h_3^{γ}	0.03	−0.36	0.26	0.96
h_4^{γ}	−0.00	−0.23	0.25	

Table 2: Results for two-dimensional fits at $\Delta \log(\mathit{Likelihood}) = 3$. In each fit all other six parameters are kept at zero.

The main sources of systematic uncertainties are considered. The influence of the angular resolution for jets and photons is found to be negligible. The uncertainty in the trigger efficiency for the $\mathrm{e^+e^-} \rightarrow \nu\bar{\nu}\gamma$ channel has a negligible impact on the limits. The systematic error due to the limited Monte Carlo statistics is computed to be 0.02 for limits on individual couplings and 0.03 for two-dimensional limits. The systematic uncertainty coming from the Monte Carlo modeling of detector inefficiencies and the resolution in the photon energy is estimated to be below 0.02. These effects are included in the limits presented.

If the data are interpreted in terms of new physics scales using formulae (1) and (2), the following limits (95% CL) to the new physics scales are obtained:

$$
\begin{array}{ll}
\Lambda_{1\mathrm{Z}} > 867~\mathrm{GeV} & \Lambda_{1\gamma} > 947~\mathrm{GeV} \\
\Lambda_{2\mathrm{Z}} > 270~\mathrm{GeV} & \Lambda_{2\gamma} > 288~\mathrm{GeV} \\
\Lambda_{3\mathrm{Z}} > 652~\mathrm{GeV} & \Lambda_{3\gamma} > 1350~\mathrm{GeV} \\
\Lambda_{4\mathrm{Z}} > 256~\mathrm{GeV} & \Lambda_{4\gamma} > 309~\mathrm{GeV}.
\end{array}
$$

To obtain these results, the maximum of the likelihood is taken at the Standard Model expectation. To determine the confidence levels the probability distributions are normalized over the physically allowed range of the parameters.

Acknowledgements

We wish to express our gratitude to the CERN accelerator divisions for the excellent performance of the LEP machine. We acknowledge the effort of the engineers and technicians who have participated in the construction and maintenance of the experiment.

References

[1] F.M. Renard, Nucl. Phys. **B 196** (1982) 93.

[2] A. Barroso *et al.*, Z. Phys. **C 28** (1985) 149.

[3] F.M. Renard, Phys. Lett. **B 126** (1983) 59.

[4] M. Claudson, E. Farhi, R.L. Jaffe, Phys. Rev. **D 34** (1986) 873.

[5] P. Mery, M. Perrotet, F.M. Renard, Z. Phys. **C 38** (1988) 579.

[6] H. Czyz, K. Kołodziej, M. Krałek, Z. Phys. **C 43** (1989) 97.

[7] U. Baur, E. Berger, Phys. Rev. **D 47** (1993) 4889.

[8] CDF Collab., F. Abe *et al.*, Phys. Rev. Lett. **74** (1995) 1941.

[9] D0 Collab., S. Abachi *et al.*, Phys. Rev. Lett. **78** (1997) 3640.

[10] D0 Collab., B. Abbott *et al.*, Phys. Rev. **D 57** (1998) 3817.

[11] G. J. Gounaris, J. Layssac and F. M. Renard, Phys. Rev. **D 61** (2000) 073013.

[12] J. Wudka, hep-ph/9606478, *The meaning of anomalous couplings* in Physics and Technology of the Next Linear Collider; eds. D. Burke and M. Peskin.

[13] L3 Collab., M. Acciarri *et al.*, Phys. Lett. **B 436** (1998) 187.

[14] DELPHI Collab., P. Abreu *et al.*, Phys. Lett. **B 423** (1998) 194.

[15] L3 Collab., B. Adeva *et al.*, Nucl. Inst. and Meth. **A289** (1990) 35;
L3 Collab., M. Chemarin *et al.*, Nucl. Inst. and Meth. **A349** (1994) 345;
L3 Collab., M. Acciarri *et al.*, Nucl. Inst. and Meth. **A351** (1994) 300;
L3 Collab., A. Adam *et al.*, Nucl. Inst. and Meth. **A383** (1996) 342.

[16] K. Hagiwara *et al.*, Nucl. Phys. **B 282** (1987) 253.

[17] S. Jadach *et al.*, hep-ph/9912214, Comp. Phys. Comm. accepted.

[18] S. Jadach, B.F.L. Ward and Z. Wąs, Comp. Phys. Comm **79** (1994) 503.

[19] F.A. Berends, R. Kleiss and R. Pittau, Nucl. Phys. **B 424** (1994) 308; Nucl. Phys. **B 426** (1994) 344; Nucl. Phys. (Proc. Suppl.) **B 37** (1994) 163;
R. Kleiss and R. Pittau, Comp. Phys. Comm. **85** (1995) 447;
R. Pittau, Phys. Lett. **B 335** (1994) 490.

[20] F.A. Berends, P.H. Daverfelt and R. Kleiss, Nucl. Phys. **B 253** (1985) 441; Comp. Phys. Comm. **40** (1986) 285.

[21] S. Jadach, W. Placzek and B.F.L. Ward, hep-ph/9608412;
S. Jadach *et al.*, 'Event Generators for Bhabha Scattering',
in 'Physics at LEP2', eds. G. Altarelli, T. Sjostrand, F. Zwirner,
(CERN, Geneva, 1996), Yellow Report CERN 96-01, Vol. 2, p. 229,
hep-ph/9602393.

[22] D. Karlen, Nucl. Phys. **B 289** (1987) 23.

[23] The L3 detector simulation is based on GEANT Version 3.15.
R. Brun *et al.*, "GEANT 3", CERN–DD/EE/84–1 (Revised), 1987.
The GHEISHA program (H. Fesefeldt, RWTH Aachen Report PITHA 85/02 (1985)) is used to simulate hadronic interactions.

[24] M. Diehl and O. Nachtmann, Z. Phys. **C 62** (1994) 397.

The L3 Collaboration:

M.Acciarri,[26] P.Achard,[19] O.Adriani,[16] M.Aguilar-Benitez,[25] J.Alcaraz,[25] G.Alemanni,[22] J.Allaby,[17] A.Aloisio,[28] M.G.Alviggi,[28] G.Ambrosi,[19] H.Anderhub,[48] V.P.Andreev,[6,36] T.Angelescu,[12] F.Anselmo,[9] A.Arefiev,[27] T.Azemoon,[3] T.Aziz,[10] P.Bagnaia,[35] A.Bajo,[25] L.Baksay,[43] A.Balandras,[4] S.V.Baldew,[2] S.Banerjee,[10] Sw.Banerjee,[10] A.Barczyk,[48,46] R.Barillère,[17] L.Barone,[35] P.Bartalini,[22] M.Basile,[9] R.Battiston,[32] A.Bay,[22] F.Becattini,[16] U.Becker,[14] F.Behner,[48] L.Bellucci,[16] R.Berbeco,[3] J.Berdugo,[25] P.Berges,[14] B.Bertucci,[32] B.L.Betev,[48] S.Bhattacharya,[10] M.Biasini,[32] A.Biland,[48] J.J.Blaising,[4] S.C.Blyth,[33] G.J.Bobbink,[2] A.Böhm,[1] L.Boldizsar,[13] B.Borgia,[35] D.Bourilkov,[48] M.Bourquin,[19] S.Braccini,[19] J.G.Branson,[39] V.Brigljevic,[48] F.Brochu,[4] A.Buffini,[16] A.Buijs,[44] J.D.Burger,[14] W.J.Burger,[32] X.D.Cai,[14] M.Campanelli,[48] M.Capell,[14] G.Cara Romeo,[9] G.Carlino,[28] A.M.Cartacci,[16] J.Casaus,[25] G.Castellini,[16] F.Cavallari,[35] N.Cavallo,[37] C.Cecchi,[32] M.Cerrada,[25] F.Cesaroni,[23] M.Chamizo,[19] Y.H.Chang,[50] U.K.Chaturvedi,[18] M.Chemarin,[24] A.Chen,[50] G.Chen,[7] G.M.Chen,[7] H.F.Chen,[20] H.S.Chen,[7] G.Chiefari,[28] L.Cifarelli,[38] F.Cindolo,[9] C.Civinini,[16] I.Clare,[14] R.Clare,[14] G.Coignet,[4] N.Colino,[25] S.Costantini,[5] F.Cotorobai,[12] B.de la Cruz,[25] A.Csilling,[13] S.Cucciarelli,[32] T.S.Dai,[14] J.A.van Dalen,[30] R.D'Alessandro,[16] R.de Asmundis,[28] P.Déglon,[19] A.Degré,[4] K.Deiters,[46] D.della Volpe,[28] E.Delmeire,[19] P.Denes,[34] F.DeNotaristefani,[35] A.De Salvo,[48] M.Diemoz,[35] M.Dierckxsens,[2] D.van Dierendonck,[2] F.Di Lodovico,[48] C.Dionisi,[35] M.Dittmar,[48] A.Dominguez,[39] A.Doria,[28] M.T.Dova,[18,♯] D.Duchesneau,[4] D.Dufournaud,[4] P.Duinker,[2] I.Duran,[40] H.El Mamouni,[24] A.Engler,[33] F.J.Eppling,[14] F.C.Erné,[2] P.Extermann,[19] M.Fabre,[46] R.Faccini,[35] M.A.Falagan,[25] S.Falciano,[35,17] A.Favara,[17] J.Fay,[24] O.Fedin,[36] M.Felcini,[48] T.Ferguson,[33] F.Ferroni,[35] H.Fesefeldt,[1] E.Fiandrini,[32] J.H.Field,[19] F.Filthaut,[17] P.H.Fisher,[14] I.Fisk,[39] G.Forconi,[14] K.Freudenreich,[48] C.Furetta,[26] Yu.Galaktionov,[27,14] S.N.Ganguli,[10] P.Garcia-Abia,[5] M.Gataullin,[31] S.S.Gau,[11] S.Gentile,[35,17] N.Gheordanescu,[12] S.Giagu,[35] Z.F.Gong,[20] G.Grenier,[24] O.Grimm,[48] M.W.Gruenewald,[8] M.Guida,[38] R.van Gulik,[2] V.K.Gupta,[34] A.Gurtu,[10] L.J.Gutay,[45] D.Haas,[5] A.Hasan,[29] D.Hatzifotiadou,[9] T.Hebbeker,[8] A.Hervé,[17] P.Hidas,[13] J.Hirschfelder,[33] H.Hofer,[48] G. Holzner,[48] H.Hoorani,[33] S.R.Hou,[50] Y.Hu,[30] I.Iashvili,[47] B.N.Jin,[7] L.W.Jones,[3] P.de Jong,[2] I.Josa-Mutuberría,[25] R.A.Khan,[18] M.Kaur,[18,◇] M.N.Kienzle-Focacci,[19] D.Kim,[35] J.K.Kim,[42] J.Kirkby,[17] D.Kiss,[13] W.Kittel,[30] A.Klimentov,[14,27] A.C.König,[30] A.Kopp,[47] V.Koutsenko,[14,27] M.Kräber,[48] R.W.Kraemer,[33] W.Krenz,[1] A.Krüger,[47] A.Kunin,[14,27] P.Ladron de Guevara,[25] I.Laktineh,[24] G.Landi,[16] K.Lassila-Perini,[48] M.Lebeau,[17] A.Lebedev,[14] P.Lebrun,[24] P.Lecomte,[48] P.Lecoq,[17] P.Le Coultre,[48] H.J.Lee,[8] J.M.Le Goff,[17] R.Leiste,[47] E.Leonardi,[35] P.Levtchenko,[36] C.Li,[20] S.Likhoded,[47] C.H.Lin,[50] W.T.Lin,[50] F.L.Linde,[2] L.Lista,[28] Z.A.Liu,[7] W.Lohmann,[47] E.Longo,[35] Y.S.Lu,[7] K.Lübelsmeyer,[1] C.Luci,[17,35] D.Luckey,[14] L.Lugnier,[24] L.Luminari,[35] W.Lustermann,[48] W.G.Ma,[20] M.Maity,[10] L.Malgeri,[17] A.Malinin,[17] C.Maña,[25] D.Mangeol,[30] J.Mans,[34] P.Marchesini,[48] G.Marian,[15] J.P.Martin,[24] F.Marzano,[35] K.Mazumdar,[10] R.R.McNeil,[6] S.Mele,[17] L.Merola,[28] M.Meschini,[16] W.J.Metzger,[30] M.von der Mey,[1] A.Mihul,[12] H.Milcent,[17] G.Mirabelli,[35] J.Mnich,[17] G.B.Mohanty,[10] P.Molnar,[8] T.Moulik,[10] G.S.Muanza,[24] A.J.M.Muijs,[2] B.Musicar,[39] M.Musy,[35] M.Napolitano,[28] F.Nessi-Tedaldi,[48] H.Newman,[31] T.Niessen,[1] A.Nisati,[35] H.Nowak,[47] G.Organtini,[35] A.Oulianov,[27] C.Palomares,[25] D.Pandoulas,[1] S.Paoletti,[35,17] P.Paolucci,[28] R.Paramatti,[35] H.K.Park,[33] I.H.Park,[42] G.Passaleva,[17] S.Patricelli,[28] T.Paul,[11] M.Pauluzzi,[32] C.Paus,[17] F.Pauss,[48] M.Pedace,[35] S.Pensotti,[26] D.Perret-Gallix,[4] B.Petersen,[30] D.Piccolo,[28] F.Pierella,[9] M.Pieri,[16] P.A.Piroué,[34] E.Pistolesi,[26] V.Plyaskin,[27] M.Pohl,[19] V.Pojidaev,[27,16] H.Postema,[14] J.Pothier,[17] D.O.Prokofiev,[45] D.Prokofiev,[36] J.Quartieri,[38] G.Rahal-Callot,[48,17] M.A.Rahaman,[10] P.Raics,[15] N.Raja,[10] R.Ramelli,[48] P.G.Rancoita,[26] A.Raspereza,[47] G.Raven,[39] P.Razis,[29] D.Ren,[48] M.Rescigno,[35] S.Reucroft,[11] S.Riemann,[47] K.Riles,[3] A.Robohm,[48] J.Rodin,[43] B.P.Roe,[3] L.Romero,[25] A.Rosca,[8] S.Rosier-Lees,[4] J.A.Rubio,[17] G.Ruggiero,[16] D.Ruschmeier,[8] H.Rykaczewski,[48] S.Saremi,[6] S.Sarkar,[35] J.Salicio,[17] E.Sanchez,[17] M.P.Sanders,[30] M.E.Sarakinos,[21] C.Schäfer,[17] V.Schegelsky,[36] S.Schmidt-Kaerst,[1] D.Schmitz,[1] H.Schopper,[49] D.J.Schotanus,[30] G.Schwering,[1] C.Sciacca,[28] D.Sciarrino,[19] A.Seganti,[9] L.Servoli,[32] S.Shevchenko,[31] N.Shivarov,[41] V.Shoutko,[27] E.Shumilov,[27] A.Shvorob,[31] T.Siedenburg,[1] D.Son,[42] B.Smith,[33] P.Spillantini,[16] M.Steuer,[14] D.P.Stickland,[34] A.Stone,[6] B.Stoyanov,[41] A.Straessner,[1] K.Sudhakar,[10] G.Sultanov,[18] L.Z.Sun,[20] H.Suter,[48] J.D.Swain,[18] Z.Szillasi,[43,¶] T.Sztaricskai,[43,¶] X.W.Tang,[7] L.Tauscher,[5] L.Taylor,[11] B.Tellili,[24] C.Timmermans,[30] Samuel C.C.Ting,[14] S.M.Ting,[14] S.C.Tonwar,[10] J.Tóth,[13] C.Tully,[17] K.L.Tung,[7] Y.Uchida,[14] J.Ulbricht,[48] E.Valente,[35] G.Vesztergombi,[13] I.Vetlitsky,[27] D.Vicinanza,[38] G.Viertel,[48] S.Villa,[11] M.Vivargent,[4] S.Vlachos,[5] I.Vodopianov,[36] H.Vogel,[33] H.Vogt,[47] I.Vorobiev,[27] A.A.Vorobyov,[36] A.Vorvolakos,[29] M.Wadhwa,[5] W.Wallraff,[1] M.Wang,[14] X.L.Wang,[20] Z.M.Wang,[20] A.Weber,[1] M.Weber,[1] P.Wienemann,[1] H.Wilkens,[30] S.X.Wu,[14] S.Wynhoff,[17] L.Xia,[31] Z.Z.Xu,[20] J.Yamamoto,[3] B.Z.Yang,[20] C.G.Yang,[7] H.J.Yang,[7] M.Yang,[7] J.B.Ye,[20] S.C.Yeh,[51] An.Zalite,[36] Yu.Zalite,[36] Z.P.Zhang,[20] G.Y.Zhu,[7] R.Y.Zhu,[31] A.Zichichi,[9,17,18] G.Zilizi,[43,¶] M.Zöller.[1]

1 I. Physikalisches Institut, RWTH, D-52056 Aachen, FRG[§]
III. Physikalisches Institut, RWTH, D-52056 Aachen, FRG[§]
2 National Institute for High Energy Physics, NIKHEF, and University of Amsterdam, NL-1009 DB Amsterdam, The Netherlands
3 University of Michigan, Ann Arbor, MI 48109, USA
4 Laboratoire d'Annecy-le-Vieux de Physique des Particules, LAPP,IN2P3-CNRS, BP 110, F-74941 Annecy-le-Vieux CEDEX, France
5 Institute of Physics, University of Basel, CH-4056 Basel, Switzerland
6 Louisiana State University, Baton Rouge, LA 70803, USA
7 Institute of High Energy Physics, IHEP, 100039 Beijing, China[△]
8 Humboldt University, D-10099 Berlin, FRG[§]
9 University of Bologna and INFN-Sezione di Bologna, I-40126 Bologna, Italy
10 Tata Institute of Fundamental Research, Bombay 400 005, India
11 Northeastern University, Boston, MA 02115, USA
12 Institute of Atomic Physics and University of Bucharest, R-76900 Bucharest, Romania
13 Central Research Institute for Physics of the Hungarian Academy of Sciences, H-1525 Budapest 114, Hungary[‡]
14 Massachusetts Institute of Technology, Cambridge, MA 02139, USA
15 KLTE-ATOMKI, H-4010 Debrecen, Hungary[¶]
16 INFN Sezione di Firenze and University of Florence, I-50125 Florence, Italy
17 European Laboratory for Particle Physics, CERN, CH-1211 Geneva 23, Switzerland
18 World Laboratory, FBLJA Project, CH-1211 Geneva 23, Switzerland
19 University of Geneva, CH-1211 Geneva 4, Switzerland
20 Chinese University of Science and Technology, USTC, Hefei, Anhui 230 029, China[△]
21 SEFT, Research Institute for High Energy Physics, P.O. Box 9, SF-00014 Helsinki, Finland
22 University of Lausanne, CH-1015 Lausanne, Switzerland
23 INFN-Sezione di Lecce and Universitá Degli Studi di Lecce, I-73100 Lecce, Italy
24 Institut de Physique Nucléaire de Lyon, IN2P3-CNRS,Université Claude Bernard, F-69622 Villeurbanne, France
25 Centro de Investigaciones Energéticas, Medioambientales y Tecnologícas, CIEMAT, E-28040 Madrid, Spain♭
26 INFN-Sezione di Milano, I-20133 Milan, Italy
27 Institute of Theoretical and Experimental Physics, ITEP, Moscow, Russia
28 INFN-Sezione di Napoli and University of Naples, I-80125 Naples, Italy
29 Department of Natural Sciences, University of Cyprus, Nicosia, Cyprus
30 University of Nijmegen and NIKHEF, NL-6525 ED Nijmegen, The Netherlands
31 California Institute of Technology, Pasadena, CA 91125, USA
32 INFN-Sezione di Perugia and Universitá Degli Studi di Perugia, I-06100 Perugia, Italy
33 Carnegie Mellon University, Pittsburgh, PA 15213, USA
34 Princeton University, Princeton, NJ 08544, USA
35 INFN-Sezione di Roma and University of Rome, "La Sapienza", I-00185 Rome, Italy
36 Nuclear Physics Institute, St. Petersburg, Russia
37 INFN-Sezione di Napoli and University of Potenza, I-85100 Potenza, Italy
38 University and INFN, Salerno, I-84100 Salerno, Italy
39 University of California, San Diego, CA 92093, USA
40 Dept. de Fisica de Particulas Elementales, Univ. de Santiago, E-15706 Santiago de Compostela, Spain
41 Bulgarian Academy of Sciences, Central Lab. of Mechatronics and Instrumentation, BU-1113 Sofia, Bulgaria
42 Laboratory of High Energy Physics, Kyungpook National University, 702-701 Taegu, Republic of Korea
43 University of Alabama, Tuscaloosa, AL 35486, USA
44 Utrecht University and NIKHEF, NL-3584 CB Utrecht, The Netherlands
45 Purdue University, West Lafayette, IN 47907, USA
46 Paul Scherrer Institut, PSI, CH-5232 Villigen, Switzerland
47 DESY, D-15738 Zeuthen, FRG
48 Eidgenössische Technische Hochschule, ETH Zürich, CH-8093 Zürich, Switzerland
49 University of Hamburg, D-22761 Hamburg, FRG
50 National Central University, Chung-Li, Taiwan, China
51 Department of Physics, National Tsing Hua University, Taiwan, China
§ Supported by the German Bundesministerium für Bildung, Wissenschaft, Forschung und Technologie
‡ Supported by the Hungarian OTKA fund under contract numbers T019181, F023259 and T024011.
¶ Also supported by the Hungarian OTKA fund under contract numbers T22238 and T026178.
♭ Supported also by the Comisión Interministerial de Ciencia y Tecnología.
♯ Also supported by CONICET and Universidad Nacional de La Plata, CC 67, 1900 La Plata, Argentina.
♢ Also supported by Panjab University, Chandigarh-160014, India.
△ Supported by the National Natural Science Foundation of China.

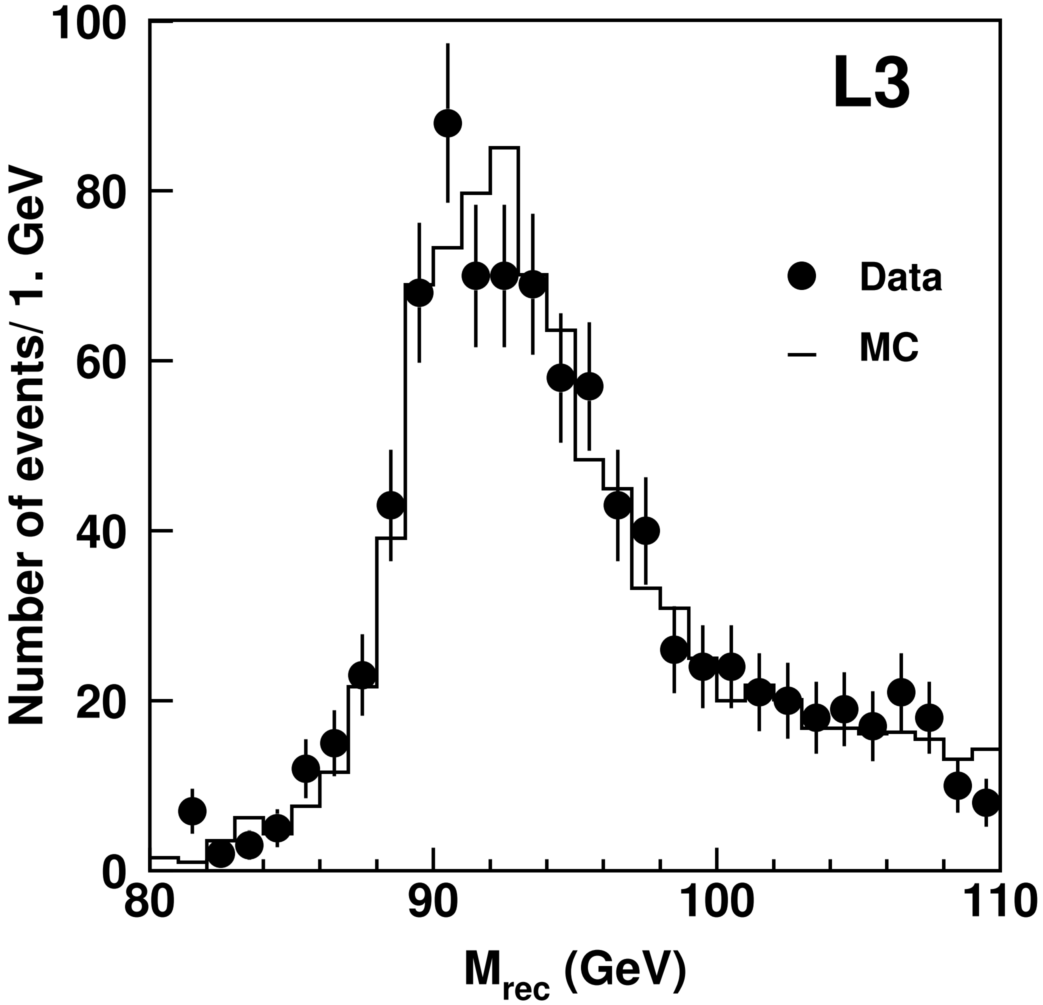

Figure 1: Distribution of the mass recoiling from the photon candidate in $e^+e^- \rightarrow q\bar{q}\gamma$ events. The points are data and the histogram is the Standard Model Monte Carlo prediction.

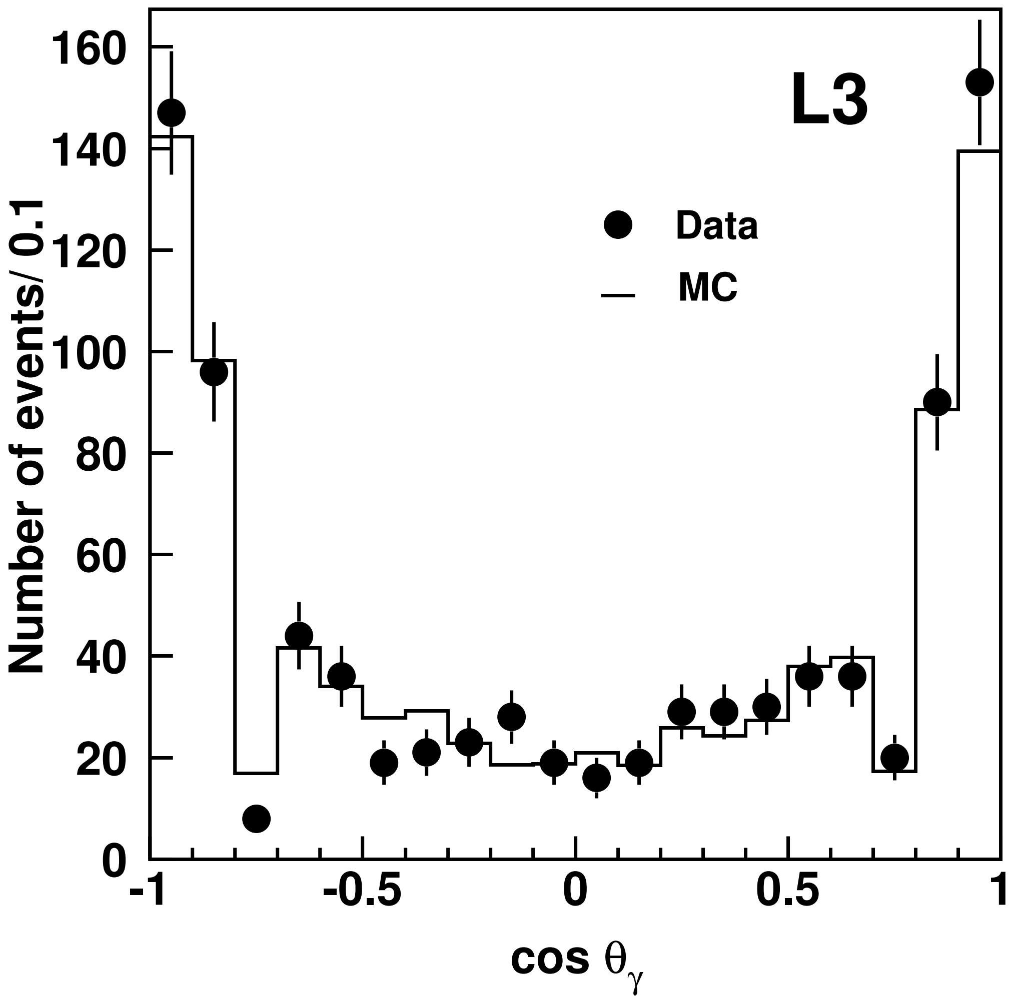

Figure 2: Polar angle distribution from the photon candidates in $e^+e^- \rightarrow q\bar{q}\gamma$ events. The points are data and the histogram is the Standard Model Monte Carlo prediction.

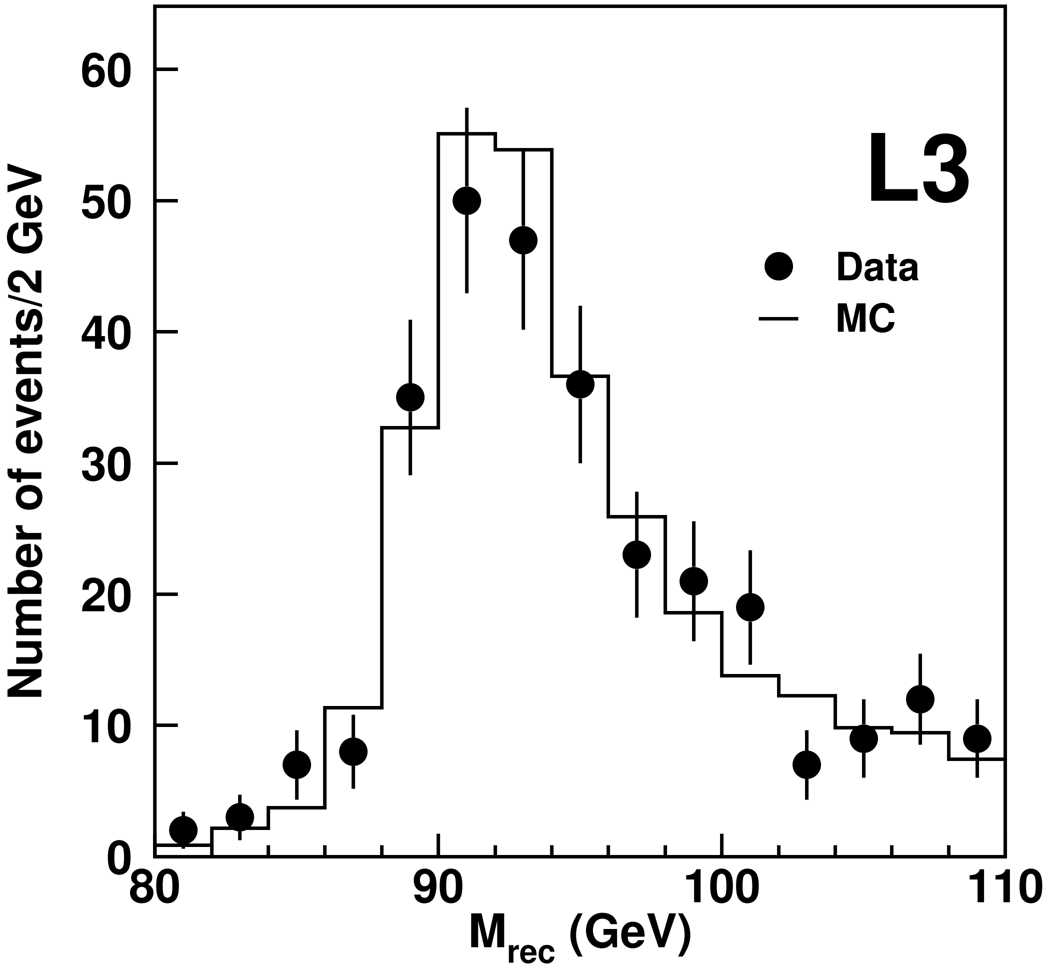

Figure 3: Distribution of the mass recoiling from the photon candidate in $e^+e^- \rightarrow \nu\bar{\nu}\gamma$ events. The points are data and the histogram is the Standard Model Monte Carlo prediction.

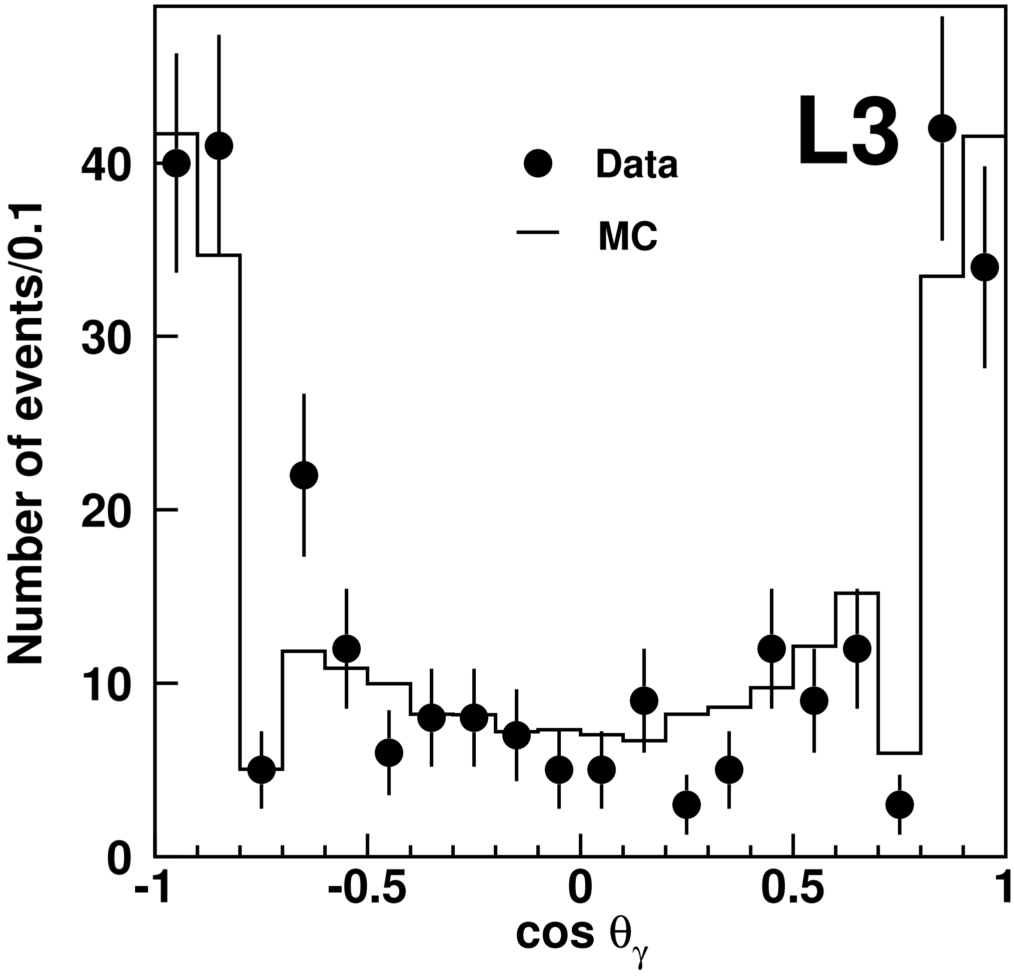

Figure 4: Polar angle distribution from the photon candidates in $e^+e^- \rightarrow \nu\bar{\nu}\gamma$ events. The points are data and the histogram is the Standard Model Monte Carlo prediction.

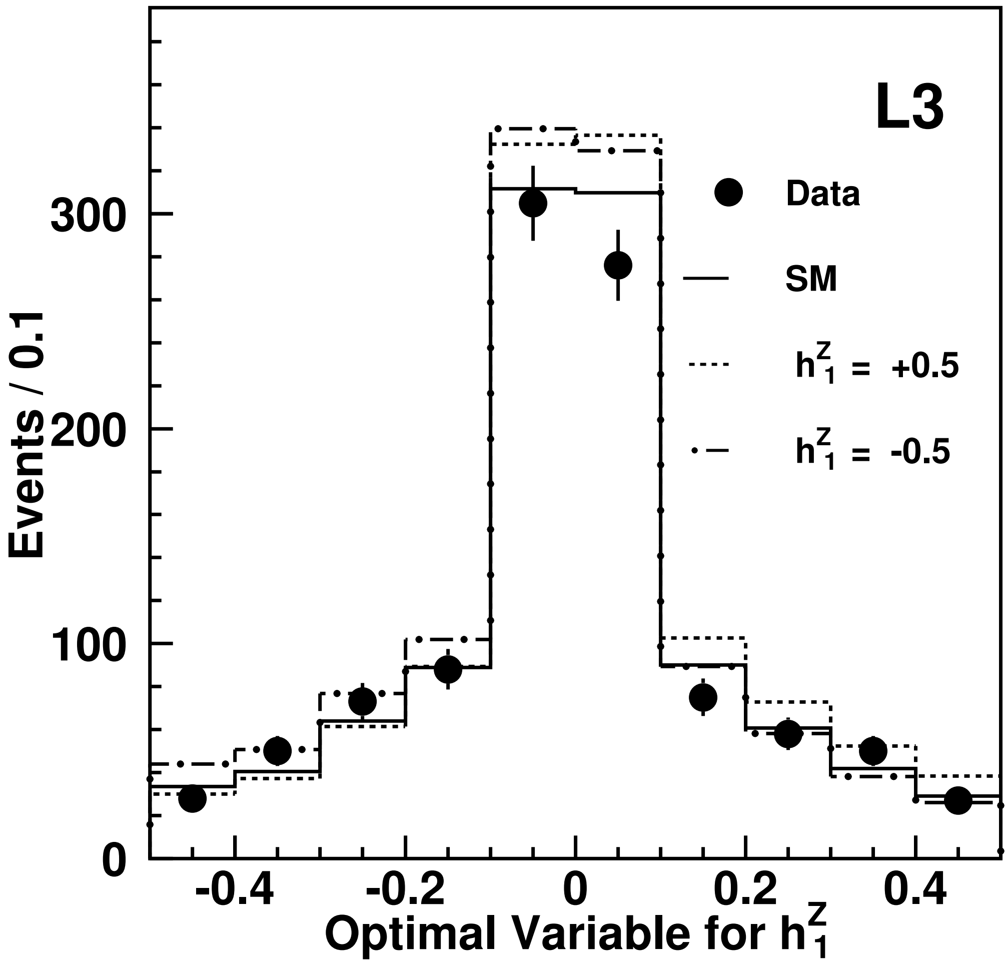

Figure 5: Distribution of the optimal variable for the CP violating coupling h_1^Z. Data are shown, together with the expectations for the Standard Model (SM) and for anomalous couplings, $h_1^Z = \pm 0.5$.

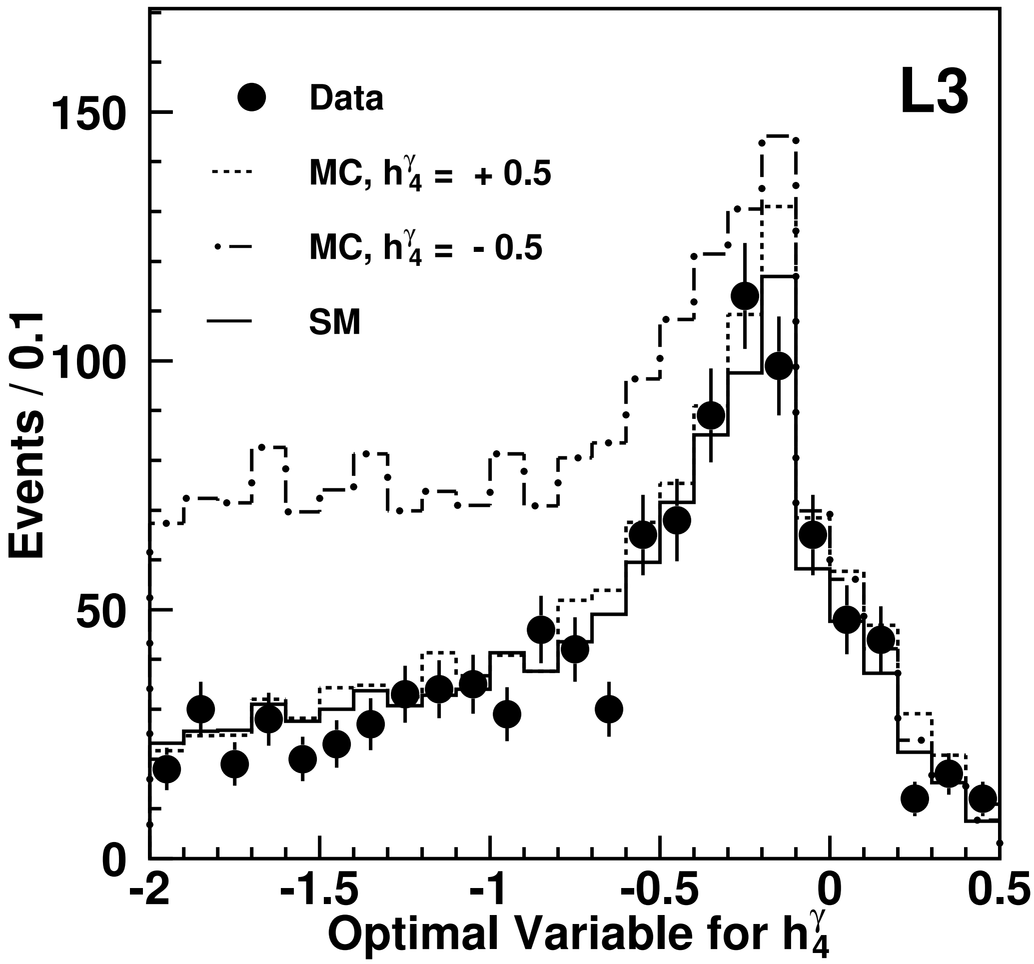

Figure 6: Distribution of the optimal variable for the CP conserving coupling h_4^γ. Data are shown, together with the expectations for the Standard Model (SM) and for anomalous couplings, $h_4^\gamma = \pm 0.5$.

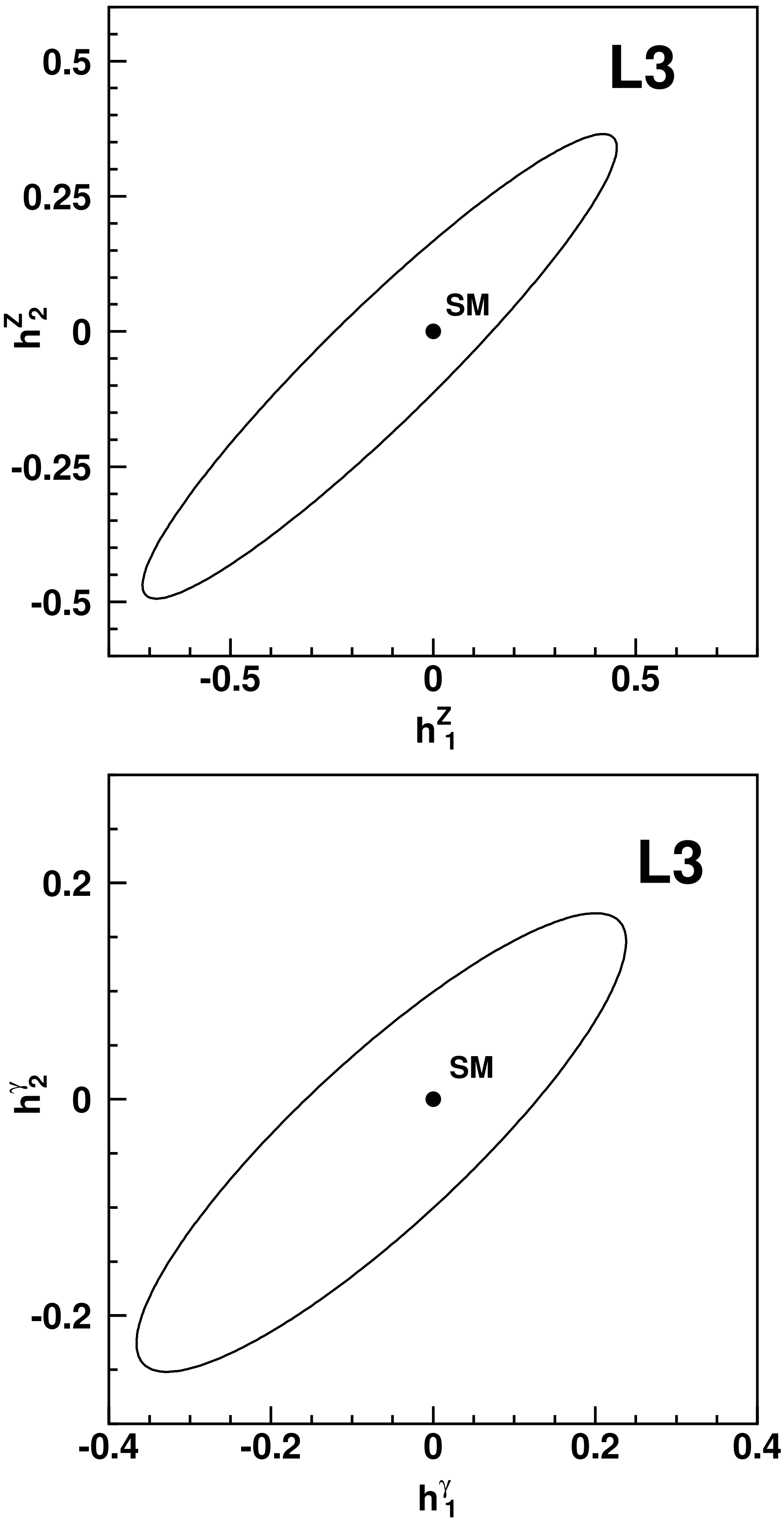

Figure 7: Limits at 95% CL on the CP-violating coupling parameters, h_2^Z versus h_1^Z and h_2^γ versus h_1^γ. The Standard Model predictions are indicated by the points. The regions outside the contours are excluded.

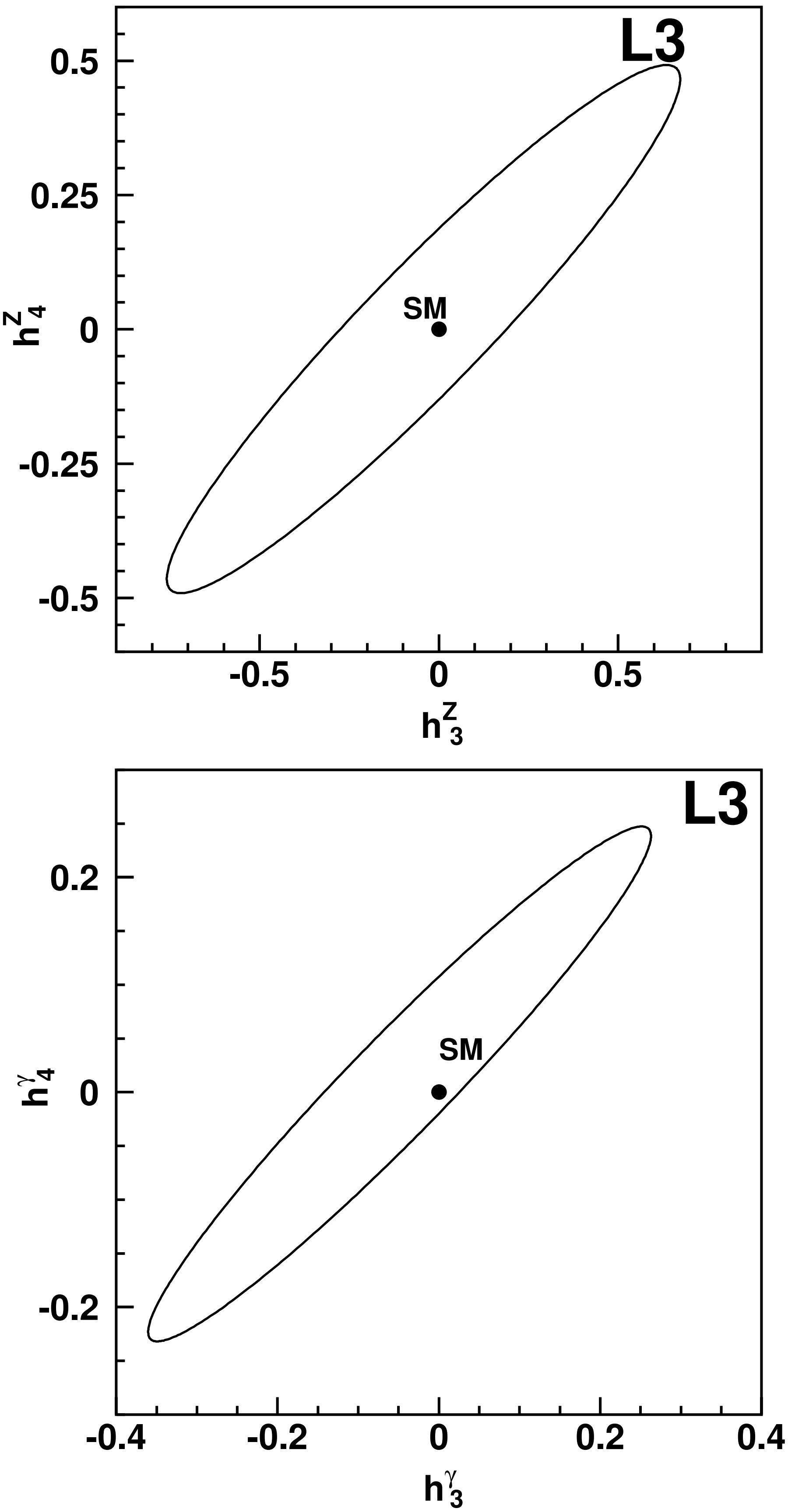

Figure 8: Limits at 95% CL on the CP-conserving coupling parameters, h_4^Z versus h_3^Z and h_4^γ versus h_3^γ. The Standard Model predictions are indicated by the points. The regions outside the contours are excluded.